Published OnlineFirst September 1, 2009; DOI: 10.1158/1535-7163.MCT-09-0662

Spotlight on Clinical Response

Activate and resist: L576P-KIT in GIST

Elena Conca,[1] Tiziana Negri,[1] Alessandro Gronchi,[2] Elena Fumagalli,[3] Elena Tamborini,[1] Giovanni Maria Pavan,[4] Maurizio Fermeglia,[4] Marco A. Pierotti,[5] Sabrina Pricl,[4] and Silvana Pilotti[1]

[1]Laboratory of Experimental Molecular Pathology, Departments of Pathology, [2]Surgery, and [3]Clinical Oncology, Fondazione Istituto Di Ricovero e Cura a Carattere Scientifico (IRCCS) Istituto Nazionale dei Tumori, Milan, Italy, [4]Molecular Simulation Engineering Laboratory, Dipartimento Ingegneria Chimica dell'Ambiente e delle Materie Prime (DICAMP), University of Trieste, Trieste, Italy, and [5]Scientific Directorate, Fondazione IRCCS Istituto Nazionale dei Tumori, Milan, Italy

Abstract

L576P is a rare *KIT* mutation often reported in cancers other than gastrointestinal stromal tumors (GIST). In GISTs, it correlates with features linked to an aggressive phenotype, eventually resulting in secondary mutations. *In vitro* findings point out that L576P/KIT is constitutively activated, and shows poor imatinib sensitivity. In this work, histological, immunohistochemical, and biochemical analyses, coupled with mutational-molecular analysis and fluorescence *in situ* hybridization, were applied to surgical specimens. In parallel, the affinities of wild-type, L576P/KIT, and Δ559/KIT for imatinib were estimated by *in silico* studies. Despite imatinib treatment and the apparent clinical-imaging response, the detected histological response was very low. KIT resulted, expressed and activated in absence of secondary mutations, *BRAF/NRAS* mutations, and *KIT/PDGFRA* gene alterations. Computer modeling proved that L576P/KIT is two times less sensitive than the wild-type counterpart and considerably less affine to imatinib than the sensitive Δ559/KIT. Accordingly, the modeling evidence strongly supports the lack of tumoral regression we observed at the histological level. [Mol Cancer Ther 2009;8(9):2491–5]

Received 7/21/09; accepted 7/31/09; published OnlineFirst 9/1/09.

Grant support: AIRC (Associazione Italiana per la Ricerca sul Cancro) grants to S. Pilotti, E. Tamborini, and S. Pricl. SIMAP grant to Dr. M.A. Pierotti.

Note: E. Conca and T. Negri contributed equally to this work. S. Pricl and S. Pilotti are senior co-authors.

Requests for reprints: Sabrina Pricl, Molecular Simulation Engineering Laboratory, DICAMP, University of Trieste, Piazzale Europa 1, 34127 Trieste, Italy. Phone: 390-405-583750; Fax: 39040569823. E-mail: sabrina.pricl@dicamp.units.it

doi:10.1158/1535-7163.MCT-09-0662

Introduction

The molecular profile of most gastrointestinal stromal tumors (GIST) is characterized by the mutually exclusive oncogenic mutation of two members of the type III tyrosine kinase receptors: KIT and PDGFRA. This finding provided the rationale for tyrosine kinase inhibitor (TKI) treatments in these tumors, which are highly resistant to conventional therapies. *KIT* mutations are the most frequently encountered activating mutations in GISTs, being present in about 80% of these malignancies. They mainly affect exon 11 in the kinase juxtamembrane domain (JMD), are mostly in heterozygous status, and include deletions, insertions, and missense mutations. Importantly, mutations in the KIT JMD are usually the most responsive to the ATP-competitive small molecule inhibitor imatinib (1, 2). Among the missense mutations identified in GISTs, Leu576Pro (L576P) is very rare, accounting for 8% of all exon 11 point mutations, which, in turn, range between 16.3 and 26.5% (2, 3).

Here we describe two cases of imatinib-treated and surgically resected GIST harboring L576P *KIT* exon 11 mutation, which, despite clinical and imaging evidence of regression, microscopically showed a low, minimal response rate in most of the tumoral deposits. These findings, supported by a concomitant molecular modeling study, point out a low imatinib affinity for the L576P/KIT.

Materials and Methods

Both paraffin-embedded and frozen materials were available from the patients treated with imatinib 400 mg/day (discontinued 24 hours before surgery). Written informed consent was obtained from the patients.

GIST Diagnosis and Genotyping

GIST diagnoses were confirmed as previously described (4). Paraffin-embedded samples were analyzed for *KIT* and *PDGFRA* mutations according to (4). Both cases showed the presence of *KIT* L576P exon 11 missense mutation.

Gene Mutation Analysis

The paraffin-embedded samples were analyzed for *KIT* and *PDGFRA* secondary mutations. Analysis was done in six tumoral deposits of the intrabdominal recurrence in case 1, and in five samples obtained from the primary tumor in case 2. Additional three cryo-preserved samples were analyzed in case 1. *BRAF* and *NRAS* gene analysis was done in one tumoral sample for each case, as previously reported (5).

Fluorescence *In situ* Hybridization Analysis

Fluorescence *in situ* hybridization (FISH) analysis was done as described in (4). Patient treatment and data

Published OnlineFirst September 1, 2009; DOI: 10.1158/1535-7163.MCT-09-0662

collection were done in accordance with the guidelines of an appropriate surveillance committee.

Results

Clinical History: Case 1

A 60-year-old male presented with a peritoneal metastasis from a high risk ileal GIST resected 1 year before. He was started on imatinib 400 mg/day, resulting in a complete remission. One year after, he developed a focal peritoneal progression and was operated on. The progressing lesion was resected, and, unexpectedly, many peritoneal implants (not visible on CT scans) were found, most of which were removed. He was further continued on imatinib 800 mg/day. Sixteen months after surgery he developed a generalized progression, which was also not responsive to sunitinib or to nilotinib. He eventually died of abdominal liver and peritoneal metastases 3 years after imatinib onset.

Clinical History: Case 2

A 70-year-old male presented with a large duodenal GIST. A preoperative treatment was started in order to avoid a major surgical procedure (pancreatic-duodenectomy). He received imatinib 400 mg/day for 10 months, obtaining a radiological response (reduction in tumor volume and density on CT scan). He was then operated on, and a conservative duodenal resection could be done. A postoperative treatment with imatinib 400 mg/day for one more year was planned.

Histological Findings: Case 1

The intrabdominal surgical debulking material consisted of six spindle cell tumoral nodules ranging from 0.5 to 3 cm in diameter. One nodule showed a moderate response, whereas the remaining five exhibited a low response rate (Fig. 1A and B). CD117 immunostaining showed dot-like immunoreactivity (Fig. 1C and D), and PDGFRA revealed a light cytoplasmic staining (data are not shown).

Histological Findings: Case 2

The primary duodenal tumor (6 × 4 × 4 cm) that was removed was completely sampled. In this case also, the pattern of tumoral growth was spindle cells. With the exception of a 1-cm^2 area in aggregate showing high response, the remaining samples showed a low response rate (Fig. 2A and B). CD117 immunostaining revealed cytoplasmic immunoreactivity (Fig. 2C), and PDGFRA exhibited a very light cytoplasmic staining (data are not shown).

Biochemical Analysis

A highly expressed and phosphorylated-activated KIT was present in the sample of case 1 (Fig. 1E), whereas in the sample of case 2, KIT was not particularly expressed, phosphorylated, and/or activated (Fig. 2D).

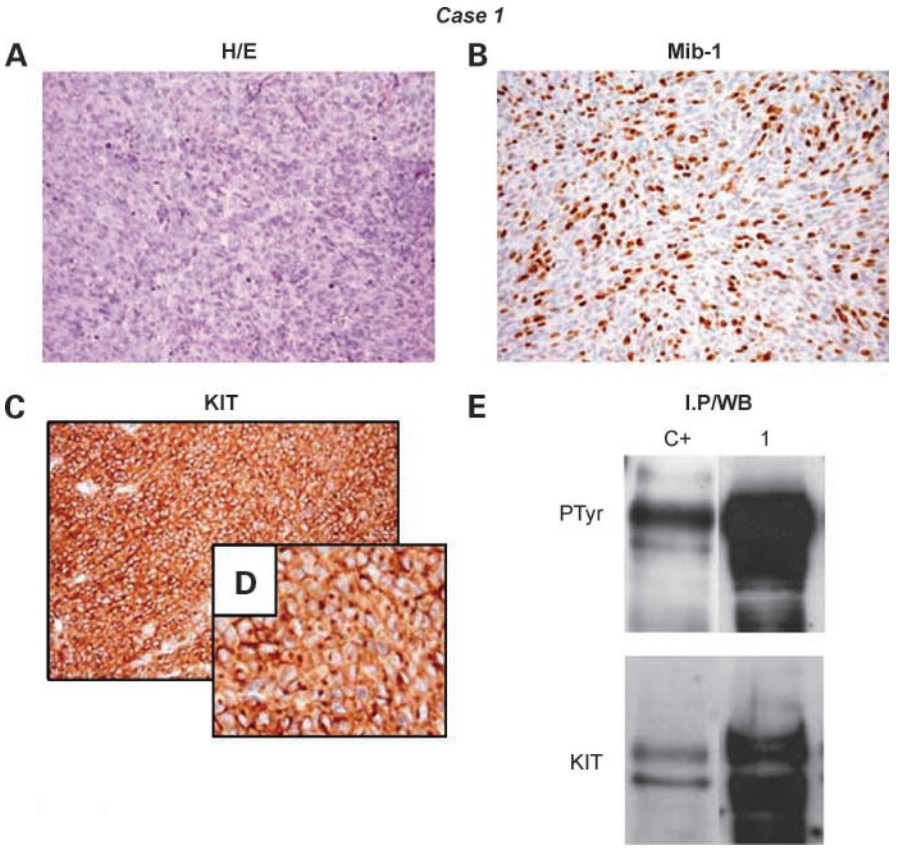

Figure 1. Case 1. Recurrence. Pathological evaluation of the post-treatment surgical tumoral specimens and biochemical findings. On fixed material, the pathological response rate was defined by averaging the residual viable tumoral cellularity, the mitotic index, and the Mib-1 labeling index (for further details see ref. 4). Briefly, a high response rate (<10 to <50% residual viable tumoral cells with no mitosis, no obvious Ki-67 immunostaining), a moderate response rate (>50–90% or >90% tumoral cells, no mitosis, Ki-67 immunostaining in 0 to <10% of cells), and a low response rate (>50–90% or >90% tumoral cells, mitotic index >10/50 HPF (high power field), Ki-67 immunostaining in 20–30% or >30% of cells) were considered. **A,** hematoxilin-eosin (H/E) and **B,** Mib-1 immunodecoration of one of the five intrabdominal nodules showing a low response rate consistent with a residual cellularity >90%; mitotic index >10/50 HPF (70/50 HPF) and a proliferation index >30%. **C,** dot-like KIT immunostaining. **D,** insert: higher power field. **E,** immunoprecipitation and Western blotting to valuate the phosphorylation-activation and expression level of KIT. In particular, 0.5 mg of protein lysates were immunoprecipitated and blotted as previously described (4), in order to verify receptor activation (anti-PTyr antibody) and expression level (anti-KIT antibody). The KIT/Δ559 cell line overexpressing an activated KIT receptor was used as positive control (C+). The sample used for biochemical analysis was characterized by a high residual cell component (residual cellularity >90%).

Published OnlineFirst September 1, 2009; DOI: 10.1158/1535-7163.MCT-09-0662

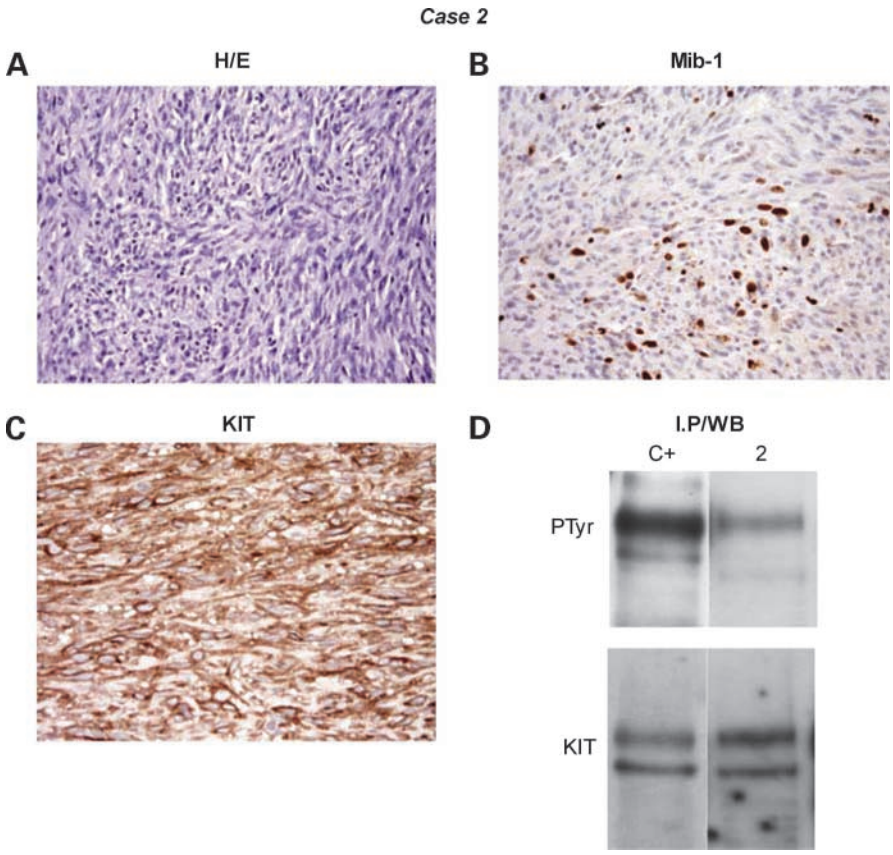

Figure 2. Case 2. Primary tumor. Pathological evaluation of the post-treatment surgical tumoral specimens and biochemical findings. **A,** hematoxilin-eosin (H/E) and **B,** Mib-1 immunodecoration of a representative sample of the primary tumor showing a low response rate consistent with a residual cellularity >90%; mitotic index >10/50HPF (13/50HPF); Ki67 labeling index ranging from <10 to >20%. **C,** cytoplasmic KIT immunostaining. **D,** immunoprecipitation and Western/blotting of KIT receptor (see legend for Fig. 1). The sample used for biochemical analysis was characterized by a high residual cell component (residual cellularity >90%).

Molecular and Molecular-Cytogenetic Findings

Neither patient carried secondary mutations. Wild-type *BRAF* and *NRAS* were found. Both cases showed a disomic pattern for *KIT* and *PDGFRA*.

Molecular Dynamic Simulations

The application of the MM-PBSA recipe to the L576P/KIT in complex with imatinib resulted in a calculated free energy of binding between inhibitor and kinase, ΔG_{bind}, of −7.75 kcal/mol. For comparison, the estimated affinity of the imatinib sensitive Δ559 isoform of KIT toward the inhibitor was ΔG_{bind} = −9.35 kcal/mol, whereas the corresponding value for the wild-type KIT was −8.08 kcal/mol. Figure 3A and B shows the equilibrated molecular dynamics (MD) models of the wild-type and L576P/KIT in complex with imatinib, respectively. Structurally, in the L576P/KIT the induced fit for imatinib binding is no longer preserved, because of a conformational change that resembles the more active form of KIT for which imatinib is known to have lower binding affinity (Fig. 3A and B).

Discussion

L576P is a rare mutation located in the JMD of KIT described in GISTs (6–10), melanomas (11), and canine GISTs and mastocytomas (12, 13). We observed three L576P mutations among 332 profiled GISTs, of which we report upon two cases here (the third being enrolled into the 62024 EORTC trial). Case 1 represents an intrabdominal recurrence of a high risk GIST arising from the ileum, whereas case 2 is a primary post-treatment high risk tumor of the duodenum. Both cases showed a low histological response score, despite the apparent clinical and imaging response.

The functional significance of L576P substitution and its imatinib sensitivity have been previously investigated on cell lines. In particular, the COS-7 cells expressing the *L576P/KIT* c-DNA revealed spontaneous KIT phosphorylation (13), and *in vitro* sensitivity tests highlighted the need of a tenfold higher dose of imatinib to switch off activated L576P/KIT with respect to V599D/KIT (11).

In terms of KIT activation, in case 1 the strong KIT expression-activation is consistent with the presence of secondary mutations that we were ultimately unable to detect, despite extensive searches with the available technique (definitely less sensitive than the recently proposed allele specific PCR; ref. 8). In case 2, the expression-activation of KIT on primary tumor was not particularly high, a finding otherwise consistent with the high heterogeneity of both KIT expression and phosphorylation previously reported in naïve and treated GISTs (6, 14). However, the evidence of post-treatment phosphorylation, along with the low rate of histological regression, support the notion that imatinib 400 mg/day was unable to switch off KIT.

In order to find a rationale for these findings, we did *"in silico"* experiments on two mutant KITs along with

Published OnlineFirst September 1, 2009; DOI: 10.1158/1535-7163.MCT-09-0662

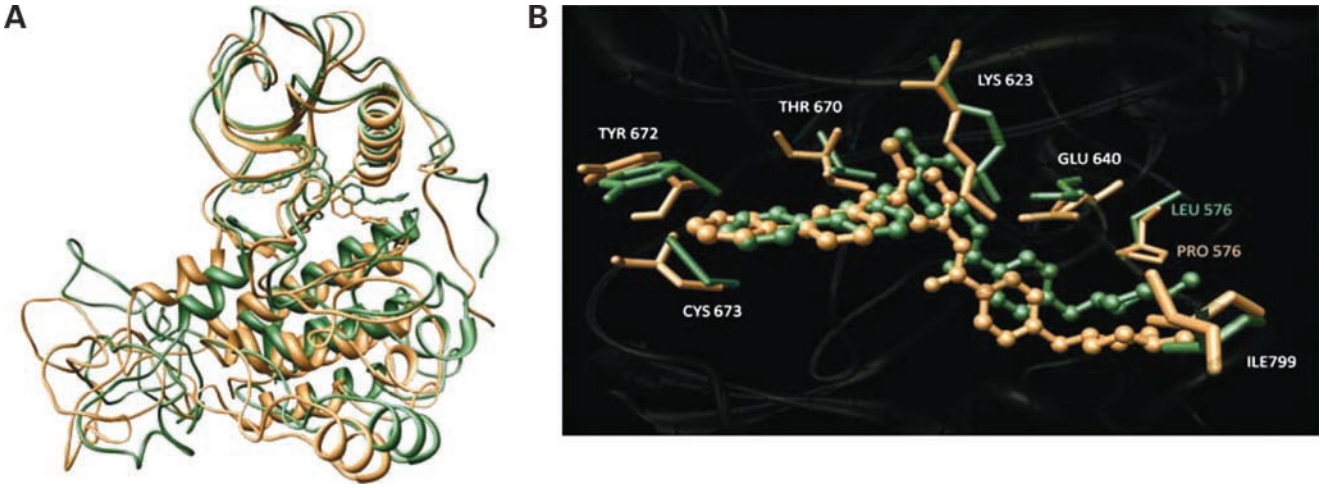

Figure 3. Computer simulations were carried out by using the AMBER 9 suite of programs (16) on 128 processors of the IBM/BCX cluster of the CINECA supercomputing facility (Bologna, Italy). The crystallographic coordinates of the inactive KIT structure in complex with imatinib (1T46.pdb; ref. 17) were employed as starting geometry. Mutations were introduced into the corresponding wild-type KIT structure, and molecular dynamics simulations were run with explicit water and counterions, according to a well-validated procedure (18, 19). The binding free energy for each kinase-inhibitor system, ΔG_{bind}, was calculated according to the Molecular Mechanics/Poisson-Boltzmann Surface Area method (MM-PBSA; ref. 20). **A,** superposition of the MD-equilibrated three-dimensional structures of wild-type (*green*) and L576P mutated KIT (*sand*) in complex with imatinib. Water molecules and counterions are omitted for clarity. **B,** details of the binding site of wild-type (*green*) and L576P mutated KIT (*sand*) in complex with imatinib. The most affected residues are depicted as sticks and labeled. Imatinib is portrayed in stick-and-ball representation. Hydrogen atoms, water molecules, and ions are omitted for clarity. In details, the L576P mutation imposes significant energetic constraints on several amino acids of the imatinib binding pocket, among which K623, E640, T670, Y672, and C673 are the most affected.

wild-type in complex with imatinib. The present MD simulations show that: (i) the L576P/KIT is considerably less affine to imatinib than the very sensitive Δ559/KIT (or V599D/KIT, as experimentally verified by Antonescu and colleagues; ref. 11), and (ii) this KIT isoform overall results in a kinase that is two times less sensitive to imatinib with respect to its wild-type counterpart. In details, our calculations confirm that the Δ559 mutant KIT is more than one order of magnitude more affine to imatinib than the naïve kinase. Indeed, when the kinase is in the closed inactive form, the only form that imatinib is able to bind to, the slight distortion induced by one residue deletion in the JMD conformation causes a conformational rearrangement that also involves the ATP-binding pocket, allowing for a larger space and, hence, a better inhibitor fitting into its binding site.

Thus, the modeling evidence gives strong support to the lack of tumoral regression that we observed at a histological level. On the basis of this study, the structural similarity of both sunitinib and nilotinib with imatinib, and the analogous binding mode to KIT of these three small molecule ATP-competitive inhibitors (data are not shown), also account for the failure of their action on L576P mutated KIT. Therefore, relying on structural homology and other direct experimental (15) and modeling evidence,[6] we can hypothesize that dasatinib, for instance, could be an effective inhibitor of L576P KIT mutant in GISTs (*in vitro* experiments are ongoing).

[6] S. Pricl, personal communications.

Disclosure of Potential Conflicts of Interest

No potential conflicts of interest were disclosed.

References

1. Corless CL, Fletcher JA, Heinrich MC. Biology of gastrointestinal stromal tumors. J Clin Oncol 2004;22:3813–25.

2. Lasota J, Miettinen M. KIT and PDGFRA mutations in gastrointestinal stromal tumors (GISTs). Semin Diagn Pathol 2006;23:91–102.

3. Lasota J, Miettinen M. Clinical significance of oncogenic KIT and PDGFRA mutations in gastrointestinal stromal tumors. Histopathology 2008;53:245–66.

4. Miselli FC, Casieri P, Negri T, et al. c-Kit/PDGFRA gene status alterations possibly related to primary imatinib resistance in gastrointestinal stromal tumors. Clin Cancer Res 2007;13:2369–77.

5. Perrone F, Da Riva L, Orsenigo M, et al. PDGFRA, PDGFRB, EGFR and downstream signalling activation in malignant peripheral nerve sheath tumour. Neuro Oncol 2009. Epub Feb 26 2009.

6. Antonescu CR, Besmer P, Guo T, et al. Acquired resistance to imatinib in gastrointestinal stromal tumor occurs through secondary gene mutation. Clin Cancer Res 2005;11:4182–90.

7. Heinrich MC, Corless CL, Blanke CD, et al. Molecular correlates of imatinib resistance in gastrointestinal stromal tumors. J Clin Oncol 2006;24:4764–74.

8. Liegl B, Kepten I, Le C, et al. Heterogeneity of kinase inhibitor resistance mechanisms in GIST. J Pathol 2008;216:64–74.

9. Debiec-Rychter M, Cools J, Dumez H, et al. Mechanisms of resistance to imatinib mesylate in gastrointestinal stromal tumors and activity of the PKC412 inhibitor against imatinib-resistant mutants. Gastroenterology 2005;128:270–9.

10. Lasota J, vel Dobosz AJ, Wasag B, et al. Presence of homozygous KIT exon 11 mutations is strongly associated with malignant clinical behavior in gastrointestinal stromal tumors. Lab Invest 2007;87:1029–41.

11. Antonescu CR, Busam KJ, Francone TD, et al. L576P KIT mutation in anal melanomas correlates with KIT protein expression and is sensitive to specific kinase inhibition. Int J Cancer 2007;121:257–64.

Published OnlineFirst September 1, 2009; DOI: 10.1158/1535-7163.MCT-09-0662

12. Frost D, Lasota J, Miettinen M. Gastrointestinal stromal tumors and leiomyomas in the dog: a histopathologic, immunohistochemical, and molecular genetic study of 50 cases. Vet Pathol 2003;40:42–54.

13. Ma Y, Longley BJ, Wang X, et al. Clustering of activating mutations in c-KIT's juxtamembrane coding region in canine mast cell neoplasms. J Invest Dermatol 1999;112:165–70.

14. Duensing A, Medeiros F, McConarty B, et al. Mechanisms of oncogenic KIT signal transduction in primary gastrointestinal stromal tumors (GISTs). Oncogene 2004;23:3999–4006.

15. Schittenhelm MM, Shiraga S, Schroeder A, et al. Dasatinib (BMS-354825), a dual SRC/ABL kinase inhibitor, inhibits the kinase activity of wild-type, juxtamembrane, and activation loop mutant KIT isoforms associated with human malignancies. Cancer Res 2006; 66:473–81.

16. Case DA, Darden TA, Cheatham TE III, et al. AMBER 9. San Francisco. San Francisco: University of California; 2006.

17. Mol CD, Dougan DR, Schneider TR, et al. Structural basis for the autoinhibition and STI-571 inhibition of c-kit tyrosine kinase. J Biol Chem 2004;279:31655–63.

18. Pricl S, Fermeglia M, Ferrone M, et al. T315I-mutated Bcr-Abl in chronic myeloid leucemia and imatinib: insights from a computational study. Mol Cancer Ther 2005;4:1167–74.

19. Negri T, Pavan GM, Virdis E, et al. T670X KIT mutations in gastrointestinal stromal tumors: making sense of missense. J Natl Cancer Inst 2009;101:194–204.

20. Srinivasan J, Cheatham TE III, Cieplak P, et al. Continuum solvent studies of the stability of DNA, RNA, and phosphoramidate-DNA helices. J Am Chem Soc 1998;120:9401–9.

AACR American Association for Cancer Research

Molecular Cancer Therapeutics

Activate and resist: L576P-KIT in GIST

Elena Conca, Tiziana Negri, Alessandro Gronchi, et al.

Mol Cancer Ther 2009;8:2491-2495. Published OnlineFirst September 1, 2009.